Molecular Microbiology (2013) 87(1), 14–29 ■
doi:10.1111/mmi.12081
First published online 19 November 2012

# Genetic requirements for *Moraxella catarrhalis* growth under iron-limiting conditions

**Stefan P. W. de Vries, Peter Burghout, Jeroen D. Langereis, Aldert Zomer, Peter W. M. Hermans and Hester J. Bootsma***
*Laboratory of Pediatric Infectious Diseases, Radboud University Medical Centre, Nijmegen, the Netherlands.*

## Summary

**Iron sequestration by the human host is a first line defence against respiratory pathogens like *Moraxella catarrhalis*, which consequently experiences a period of iron starvation during colonization. We determined the genetic requirements for *M. catarrhalis* BBH18 growth during iron starvation using the high-throughput genome-wide screening technology genomic array footprinting (GAF). By subjecting a large random transposon mutant library to growth under iron-limiting conditions, mutants of the MCR_0996-*rhlB*-*yggW* operon, *rnd*, and MCR_0457 were negatively selected. Growth experiments using directed mutants confirmed the GAF phenotypes with Δ*yggW* (putative haem-shuttling protein) and ΔMCR_0457 (hypothetical protein) most severely attenuated during iron starvation, phenotypes which were restored upon genetic complementation of the deleted genes. Deletion of *yggW* resulted in similar attenuated phenotypes in three additional strains. Transcriptional profiles of Δ*yggW* and ΔMCR_0457 were highly altered with 393 and 192 differentially expressed genes respectively. In all five mutants, expression of nitrate reductase genes was increased and of nitrite reductase decreased, suggesting an impaired aerobic respiration. Alteration of iron metabolism may affect nasopharyngeal colonization as adherence of all mutants to respiratory tract epithelial cells was attenuated. In conclusion, we elucidated the genetic requirements for *M. catarrhalis* growth during iron starvation and characterized the roles of the identified genes in bacterial growth and host interaction.**

Accepted 20 October, 2012. *For correspondence. E-mail H.Bootsma@cukz.umcn.nl; Tel. (+31) 24 3666332; Fax (+31) 24 3666352.



## Introduction

*Moraxella catarrhalis* is an emerging pathogen of the human upper and lower respiratory tract. This Gram-negative bacterium colonizes the upper respiratory tract with a high frequency in infants; approximately two-thirds of this population becomes colonized within their first year of life. Importantly, *M. catarrhalis* is the third most common cause of childhood otitis media (OM) after *Streptococcus pneumoniae* and *Haemophilus influenzae*. Further, *M. catarrhalis* is responsible for about 10–15% of the exacerbations in patients suffering from chronic obstructive pulmonary disease (COPD) (Sethi and Murphy, 2008; Perez Vidakovics and Riesbeck, 2009; de Vries *et al*., 2009).

Iron is an essential nutrient throughout all kingdoms of life. It acts as a cofactor in various cellular processes including aerobic respiration, DNA metabolism and the oxidative stress response (Ratledge and Dover, 2000). Because the host is devoid of free iron, all bacterial pathogens will encounter a period of iron starvation. In line with this, sensing iron depletion can serve as an indicator of host tissue (Skaar, 2010). In the human host, iron is sequestered by high-affinity iron-binding proteins such as lactoferrin, transferrin, haemoglobin and haem. The process of iron sequestration is an important line of defence against invading bacterial pathogens, a process which is also referred to as nutritional immunity (Skaar, 2010). To counteract this nutritional immunity, *M. catarrhalis* expresses several iron-acquisition systems that allows it to extract iron from host iron-sequestration proteins such as the lactoferrin- and transferrin-binding proteins LbpA/B and TbpA/B and the outer membrane protein CopB, linked to iron acquisition from both lactoferrin and transferrin, reviewed in de Vries *et al*. (2009). Upon iron starvation, *M. catarrhalis* alters its gene expression to enhance acquisition of iron, e.g. expression of genes encoding LbpA/B, TbpA/B and CopB is increased, as is expression of iron-transport factors such as the inner membrane complex TonB–ExbB–ExbD (Aebi *et al*., 1996; Wang *et al*., 2007).

Importantly, differential gene expression does not always directly translate into gene essentiality, and reversely, genes that are required for growth under iron-limiting conditions are not necessarily differentially expressed upon iron starvation. To assess whether a gene

is conditionally essential, specific gene deletions or disruptions are commonly used. Hansen and co-workers clearly demonstrated the applicability of transposon mutagenesis to identify genes essential for biofilm formation of *M. catarrhalis* in a comprehensive fashion (Pearson *et al*., 2006; Pearson and Hansen, 2007). In these studies, a large number of transposon mutants were tested individually to determine their biofilm-formation phenotype. At present, however, no high-throughput method is available that allows screening of a large number of *M. catarrhalis* mutants simultaneously.

Here, we report the adaptation and improvement of the genomic array footprinting (GAF) technology to identify conditionally essential genes in *M. catarrhalis*. GAF, originally developed for *S. pneumoniae* (Bijlsma *et al*., 2007; Burghout *et al*., 2007; Molzen *et al*., 2011), is a high-throughput genome-wide negative selection screenings method that combines *marinerT7* transposon mutagenesis with microarray technology to identify mutants that are negatively selected from a library due to a particular challenge or stress condition. We have used GAF to gain insight into the genetic requirements for *M. catarrhalis* growth under iron-limiting conditions, in this way mimicking a stress condition that the pathogen faces inside the human host. The requirement of the identified genes in iron starvation was validated using directed gene deletion mutants and genetic complementation. Finally, functional characterization of the newly identified genes was performed by exposure to various peroxides, adhesion to respiratory tract epithelial cells and microarray expression profiling.

## Results

### *Genome-wide identification of genes essential for growth under iron-limiting conditions*

To identify genes that are essential for *M. catarrhalis* growth under iron-limiting conditions, we used an adapted version of the GAF technology (Fig. 1). To this end, a large *marinerT7* transposon mutant library (~ 28 000 independent transposon mutants) of strain BBH18 was grown under iron-limiting conditions, achieved by sequestration of iron by Desferal, and under control growth conditions. Transposon mutants were recovered during the exponential and early-stationary growth phase. Notably, under iron-limiting conditions growth of the mutant library was reduced to approximately 50% of the growth in the control condition (Fig. 1B), which implies that our challenge condition was sufficiently stringent to negatively select for iron-dependent mutants. To improve the readout of the challenged and control mutant libraries with GAF microarrays, we made several important modifications to the original GAF procedure developed for *S. pneumoniae*. First, we redesigned the set-up of the GAF microarrays by using single-stranded oligonucleotide probes of 50–72 nucleotides (nt) in length, spaced about 200 base pairs (bp) apart on both strands of the reference genome. Second, we implemented an actinomycin D-based protocol for the asymmetrical generation of single-stranded mutant-specific cDNA probes. With these improvements, we could map the location of a transposon insertion site to a 200 bp region of the target genome, as shown in Fig. 1C and D. Changes in the probe signal intensities (SI) adjacent to the transposon insertion site in the challenge versus the control growth condition indicated conditional attenuation or enrichment of transposon mutants.

In total, eight transposon insertion mutants corresponding to five genes were negatively selected from the library during growth under iron-limiting conditions, while one mutant appeared to be enriched (Table 1). The largest change in GAF signal was observed for mutants of the *yggW* gene, predicted to be involved in the biosynthesis of haem (formation of protoporphyrinogen) based on homology to HemN family coproporphyrinogen-III oxidase proteins. Furthermore, we identified the *rhlB* and MCR_0996 genes located adjacent to *yggW*, which are predicted to encode an ATP-dependent RNA helicase and a hypothetical protein respectively. The other transposon insertions which reduced growth under iron-limiting conditions were in the *rnd* gene (MCR_0843, ribonuclease D) and the MCR_0457 gene encoding a hypothetical protein. All of the identified genes were found to be highly conserved across *M. catarrhalis* clinical isolates (de Vries *et al*., 2010; Davie *et al*., 2011), with levels of identity ranging from 99% to 100% (data not shown).

### *Characterization of identified genes in BBH18 and other* M. catarrhalis *isolates: phenotypic validation, chemical and genetic complementation*

To validate the attenuated GAF phenotypes, directed gene deletion mutants of all five identified genes were generated in *M. catarrhalis* BBH18. In addition, we included mutants of *M. catarrhalis* genes encoding the known iron-acquisition factors CopB (Aebi *et al*., 1996) and LbpA (Du *et al*., 1998), which were not identified in this GAF screen. Growth rate constants (generations per hour) of all directed mutants were determined. Under control growth conditions all mutants displayed wild-type growth characteristics (Fig. 2A and Fig. S1). However, under iron-limiting conditions Δ*yggW* and ΔMCR_0457 did not survive, and growth of Δ*rhlB*, ΔMCR_0996 and Δ*rnd* was significantly attenuated (Fig. 2B and Fig. S1). Importantly, the Δ*copB* and Δ*lbpA* strains did not show differential growth under iron-limiting conditions (Fig. 2B and Fig. S1), which is consistent with the fact that they were not negatively selected from the mutant library during our GAF screen. To confirm that the attenuated

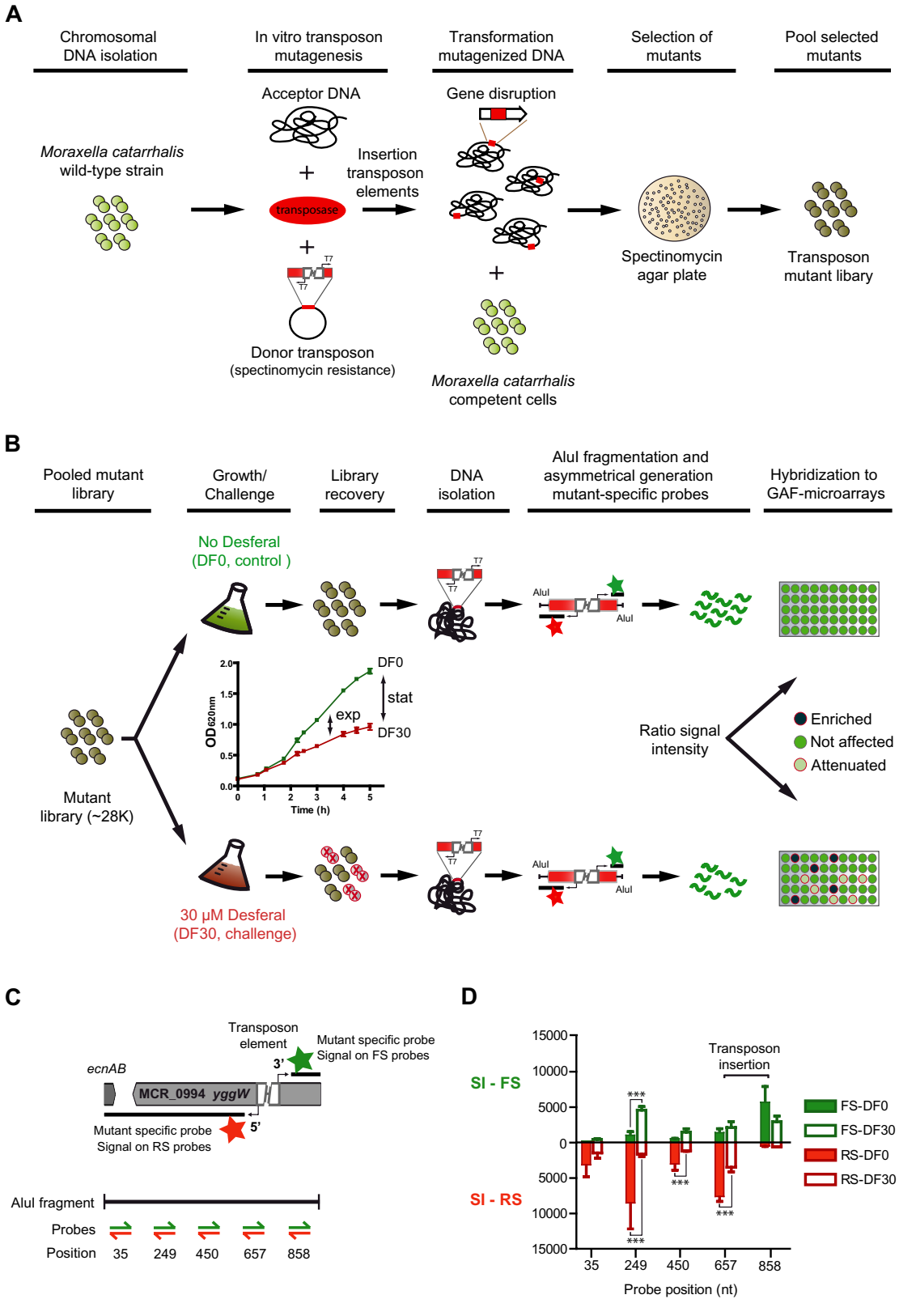
A
Chromosomal DNA isolation
In vitro transposon mutagenesis
Transformation mutagenized DNA
Selection of mutants
Pool selected mutants
Moraxella catarrhalis wild-type strain
Acceptor DNA
transposase
Insertion transposon elements
Donor transposon (spectinomycin resistance)
Gene disruption
Moraxella catarrhalis competent cells
Spectinomycin agar plate
Transposon mutant libary
B
Pooled mutant library
Growth/ Challenge
Library recovery
DNA isolation
AluI fragmentation and asymmetrical generation mutant-specific probes
Hybridization to GAF-microarrays
No Desferal (DF0, control )
30 µM Desferal (DF30, challenge)
Mutant library (~28K)
OD620nm
Time (h)
DF0
DF30
stat
exp
AluI
Ratio signal intensity
Enriched
Not affected
Attenuated
C
Transposon element
Mutant specific probe Signal on FS probes
ecnAB
MCR_0994 yggW
3'
5'
Mutant specific probe Signal on RS probes
AluI fragment
Probes
Position 35 249 450 657 858
D
SI - FS
SI - RS
Transposon insertion
FS-DF0
FS-DF30
RS-DF0
RS-DF30
Probe position (nt)

**Fig. 1.** Genomic array footprinting (GAF).
A. GAF flow scheme. Chromosomal DNA of *M. catarrhalis* strain BBH18 is isolated and used as acceptor DNA in an *in vitro marinerT7* transposition reaction. Integration of the *marinerT7* transposon element in TA sites results in random disruption of genes. *In vitro* mutagenized DNA is transformed into competent *M. catarrhalis* BBH18 cells, and transposon mutants are selected on spectinomycin-containing agar plates. The mutant library is prepared by pooling of ~ 28 000 single colonies.
B. Experimental set-up for iron limitation GAF screen. The *marinerT7* transposon mutant library was grown under either control or iron-limiting conditions (challenge), after which T7 RNA was generated from DNA of recovered mutants and used for the asymmetrical generation of Cy3-labelled mutant-specific probes that were hybridized to custom-designed Nimblegen microarrays. Mutants that failed to survive under iron-limiting conditions were identified by differential hybridization patterns.
C. Strand-specific probe generation. AluI-digested chromosomal DNA of recovered mutants was used for the asymmetrical generation of Cy3-labelled forward strand and reverse strand mutant-specific probes by *in vitro* transcription of the T7 promoter at the end of the *marinerT7* transposon. The *yggW* AluI fragment is shown as an example.
D. GAF analysis. Asymmetrically generated mutant-specific cDNA probes were hybridized to GAF microarrays designed based on AluI restriction fragments, with single-stranded oligonucleotide probes spaced every ~ 200 bp on both strands. For the *yggW* AluI fragment shown here, the highest signals intensities (SI) were observed on the reverse strand (RS) probes (red bars) located at position 35, 249, 450 and 657, whereas on position 858 the SI was higher on the forward strand (FS) probes (green bars), indicating the presence of a transposon element between position 657 and 858, disrupting *yggW*. Iron starvation resulted in loss of mutant-specific probe signal, indicating that *yggW* is essential for growth under this condition. Triple asterisks (***) denote statistically significance difference between SI of DF0 and DF30 ($P_{bayes}$ < 0.001 and FDR < 0.01). Graph shows means and standard error of the mean (SEM) ($n$ = 4).

growth was the effect of the reduced availability of iron, mutants were grown under iron-repleted conditions, created through the addition of iron sulphate (Fig. 2C and Fig. S1) and haemin (Fig. 2D and Fig. S1). Growth of *yggW, rhlB*, MCR_0996 and *rnd* mutants was completely restored to wild-type levels after iron repletion, while growth of ΔMCR_0457 was partially restored.

The most prominent growth defects under iron-limiting conditions were observed after deletion of *yggW* and MCR_0457 in *M. catarrhalis* BBH18. To confirm that the observed phenotypes were indeed due to the gene deletions, we generated genetically complemented mutants by expression of the respective genes from the plasmid pSV001. To ensure expression, the *yggW* gene (lacking a likely promoter sequence directly upstream) was fused to the *bro-1* promoter, while for MCR_0457 the predicted native promoter was included. Real-time quantitative PCR (RT-qPCR) analysis showed that expression of both genes was completely restored, and even 4- to 10-fold higher than wild-type (Fig. 3A). Importantly, growth of the complemented ΔMCR_0457 mutant under iron-limiting conditions was indistinguishable from wild-type (Fig. 3C). The *yggW* mutant showed near wild-type levels of growth upon genetic complementation, possibly the result of both the severe phenotype of the gene deletion mutant and the relatively high *yggW* expression in the complemented mutant (Fig. 3B).

To examine whether the importance of *yggW* and MCR_0457 for growth during iron starvation is conserved across *M. catarrhalis* isolates, we deleted these genes in three other strains, namely O35E, 7169 and 46P47B1. Since these wild-type strains turned out to be more sensitive to Desferal than the BBH18 strain (data not shown), we examined growth in BHI pre-treated 20 μM Desferal. In all three strains deletion of *yggW* results in attenuated growth during iron starvation (Fig. 3D–F), indicating a conserved role of *yggW* across the *M. catarrhalis* species. No effects of the MCR_0457 deletion were observed, although a minor attenuation was observed in strain 7169 and 46P47B1, albeit not statistically significant.

**Table 1.** Genes that play a role during growth under iron-limiting conditions.[a]

| | | | | Exponential phase | | | Early-stationary phase | | |
|---|---|---|---|---|---|---|---|---|---|
| Locus_tag | Gene | Description | AluI fragment | DF0/DF30 | $P_{bayes}$ | FDR | DF0/DF30 | $P_{bayes}$ | FDR |
| MCR_0457 | | Hypothetical protein | 474102.474292 | 1.9 | 1.2E-09 | 1.9E-06 | | | |
| MCR_0843 | *rnd* | Ribonuclease D | 847210.847362 | 2.1 | 9.9E-09 | 1.0E-05 | | | |
| MCR_0994 | *yggW* | Oxygen-independent coproporphyrinogen-III | 992384.9993292 | 3.2 | 1.1E-05 | 8.5E-04 | 2.8 | 8.5E-06 | 4.0E-03 |
| | | | 993293.993517 | 1.9 | 2.5E-12 | 2.5E-08 | | | |
| | | oxidase-like protein | 993518.994377 | 2.3 | 5.8E-10 | 8.7E-07 | 2.1 | 6.8E-07 | 1.5E-03 |
| MCR_0995 | *rhlB* | ATP-dependent RNA helicase | 994654.994894 | 2.2 | 7.5E-09 | 8.4E-06 | | | |
| MCR_0996 | | Hypothetical protein | 994896.995101 | 2.1 | 1.3E-11 | 6.6E-08 | | | |
| | | | 995301.995509 | 2.0 | 1.9E-10 | 3.7E-07 | 1.9 | 1.3E-06 | 2.8E-03 |
| MCR_0112 | *purL* | Phosphoribosyl-formylglycinamidine synthase | 126308.127090 | | | | –2.0 | 2.8E-06 | 4.3E-03 |

**a.** Differential cut-off criteria: fold-change > 1.9, $P_{bayes}$ < 0.001, false discovery rate (FDR) < 0.01. Values given are the average values of the probes that met the selection criteria.

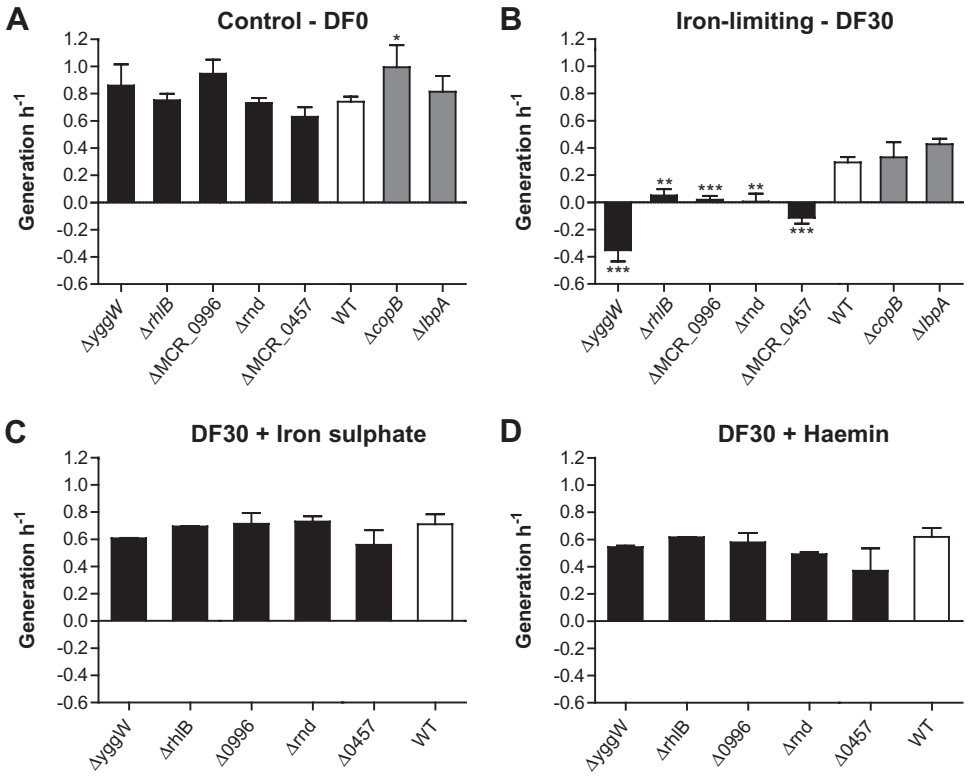


**Fig. 2.** *In vitro* growth characteristics of BBH18 directed gene deletion mutant strains. Mutants were cultured under control (A, BHI-DF0), iron-limiting (B, BHI-DF30) and iron-repleted (C: BHI-DF30 supplemented with 100 μM iron sulphate; D: BHI-DF30 supplemented with 20 μM haemin) conditions. The growth speed (generations per hour) of the mutant and wild-type (WT) strains was determined during exponential growth. Growth of directed mutant strains was severely affected under iron-limiting conditions and completely restored upon iron repletion via the addition of iron sulphate and haemin, although no full rescue was observed for the MCR_0457 mutant. Statistical difference with the wild-type strains under control and iron-limiting conditions ($n \geq 3$) (A and B) was determined with a Mann–Whitney test. Statistical analysis for growth in iron-repleted medium ($n = 2$) (C and D) was determined with an unpaired *t*-test with Welch's correction. For all experiments, data shown are means and SEM. $^{*}P < 0.05$, $^{**}P < 0.01$, $^{***}P < 0.001$.

The genetic structure of the MCR_0996-*rhlB-yggW* cluster suggests that it functions as an operon (Fig. 4A). Gene-spanning PCR reactions on BBH18 cDNA demonstrated that this gene cluster is indeed transcribed as a polycistronic messenger (Fig. 4B). For each individual deletion mutant of the MCR_0996-*rhlB-yggW* operon genes, we confirmed that expression of the other two operon genes was not affected (Fig. 4C), ruling out that polar effects caused the attenuated growth phenotypes under iron-limiting conditions.

There is a link between iron metabolism and oxidative stress as the reaction of iron with peroxide (i.e. Fenton reaction) results in the generation of highly reactive oxygen species (ROS). In this light, we assessed the sensitivity of the directed mutants to the oxidative agents hydrogen peroxide, tert-butyl peroxide, cumene hydroperoxide and tellurite (Whitby *et al.*, 2010; Hoopman *et al.*, 2011). However, none of the mutants displayed increased sensitivity for the tested peroxides and tellurite (data not shown).

### *Link between iron metabolism and adherence to respiratory tract epithelial cells*

Next to acquiring essential nutrients such as iron, *M. catarrhalis* also needs to be able to adhere to the epithelial cell layer, as this is a critical first step towards colonization and infection. Therefore, we tested the ability of the directed mutants to adhere to two human respiratory tract epithelial cell lines, Detroit 562 pharyngeal and A549 type-II alveolar epithelial cells. Since the deletion mutants were attenuated for growth under iron-limiting conditions, aliquots for adherence were prepared in standard BHI medium. Compared with wild-type, adhesion of all mutants to both Detroit 562 and A549 cells was significantly reduced, similar to the reduction that was observed for a mutant of the major adhesin of *M. catarrhalis uspA1* (Aebi *et al.*, 1998) (Fig. 5A and B). This adhesion defect was not caused by a growth defect of the mutants in the infection medium used for the adhesion assay (data not shown). Neither was it the result of our mutagenesis

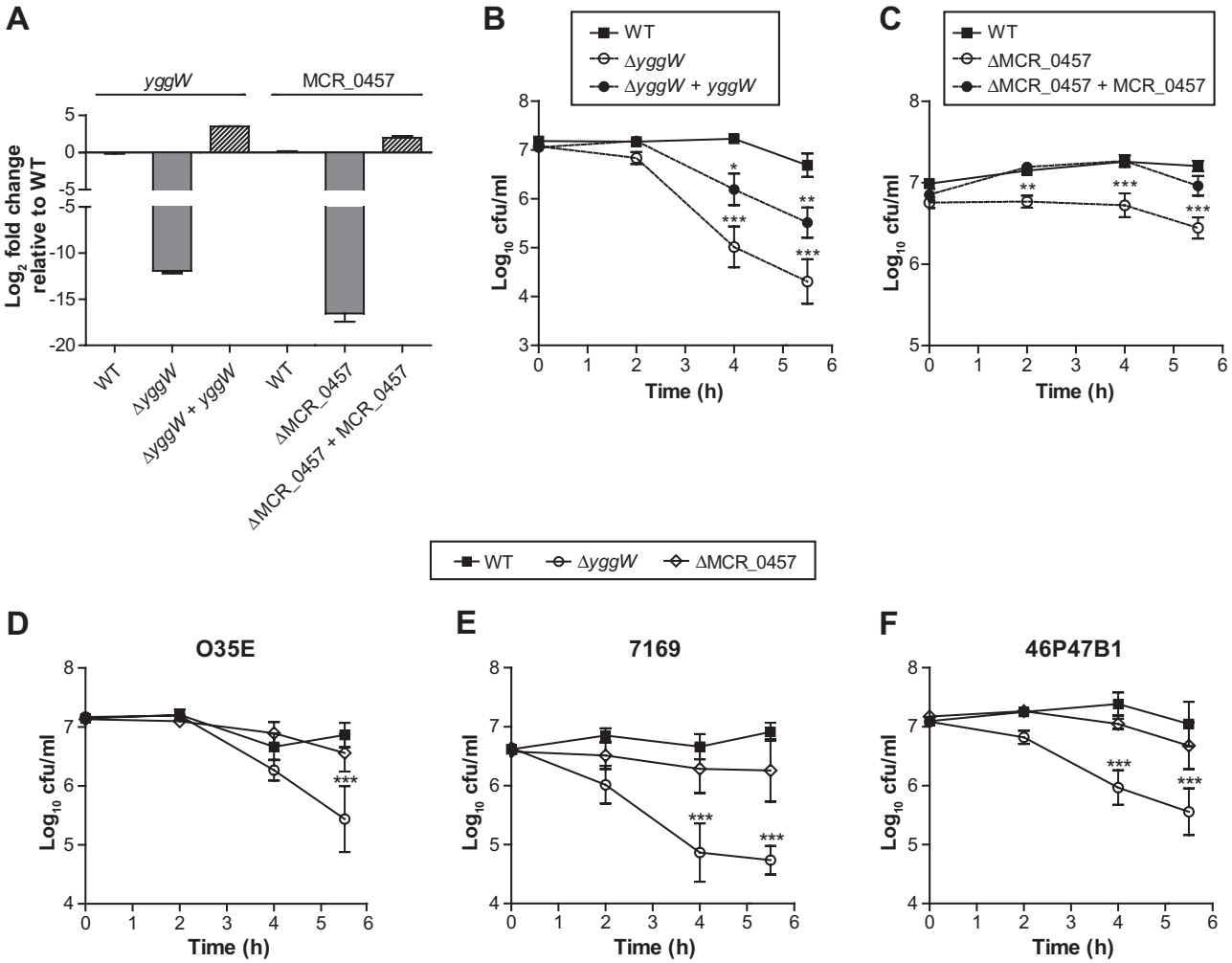


**Fig. 3.** Genetic complementation of *yggW* and MCR_0457 mutants and directed gene deletions in other *M. catarrhalis* isolates.
A. Real-time quantitative PCR analysis showed that *yggW* and MCR_0457 gene expression was restored in genetically complemented BBH18 mutant strains. Data are expressed as $\log_2$ fold-change relative to wild-type. Graphs shows mean and SEM based on analysis of three biological replicates.
B and C. Growth under iron-limiting conditions of the *yggW* and MCR_0457 mutants genetically complemented with pSV002 and pSV003 respectively ($n \geq 5$). The severe attenuation of Δ*yggW* was restored, although partially, by *trans* expression of *yggW*, i.e. significantly higher than Δ*yggW* but lower as compared with the wild-type strain. The attenuated growth of the ΔMCR_0457 mutant was completely rescued upon genetic complementation.
D–F. Growth of *yggW* and MCR_0457 mutants of strains O35E, 7169 and 46P47B1 under iron-limiting conditions (DF20) ($n = 4$). In all three tested strains deletion of *yggW* resulted in attenuated growth during iron starvation. Growth was only slightly inhibited after deletion of MCR_0457 in strains 7169 and 46P47B1.
Statistical significance (B–F) was tested on $\log_{10}$-transformed data with a two-way ANOVA and the Bonferroni *post hoc* test. $^*P < 0.05$, $^{**}P < 0.01$; $^{***}P < 0.001$. Data shown are means and SEM.

approach, as the adhesion levels of a mutant of the *olpA* gene was unaffected, which is consistent with a previous study (Brooks *et al*., 2007) (Fig. 5A and B). Examination of the outer membrane protein composition of wild-type and the mutant strains (Fig. 5C) did not reveal obvious differences, and expression of UspA1 was detected in all mutant strains (Fig. 5D), indicating that the observed defect in epithelial cell adherence of the mutants was not due to changes in outer membrane composition or alteration of known adhesion factors. Importantly, adhesion of the *yggW* and MCR_0457 mutants was restored to wild-type levels upon genetic complementation, confirming that the diminished adherence was indeed the result of the deletion of these genes (Fig. 5A and B).

### *Effect of gene deletions on transcriptional profiles*

To further characterize the functional consequences of the gene deletions, we determined transcriptome profiles of the wild-type and directed mutant strains during exponen-

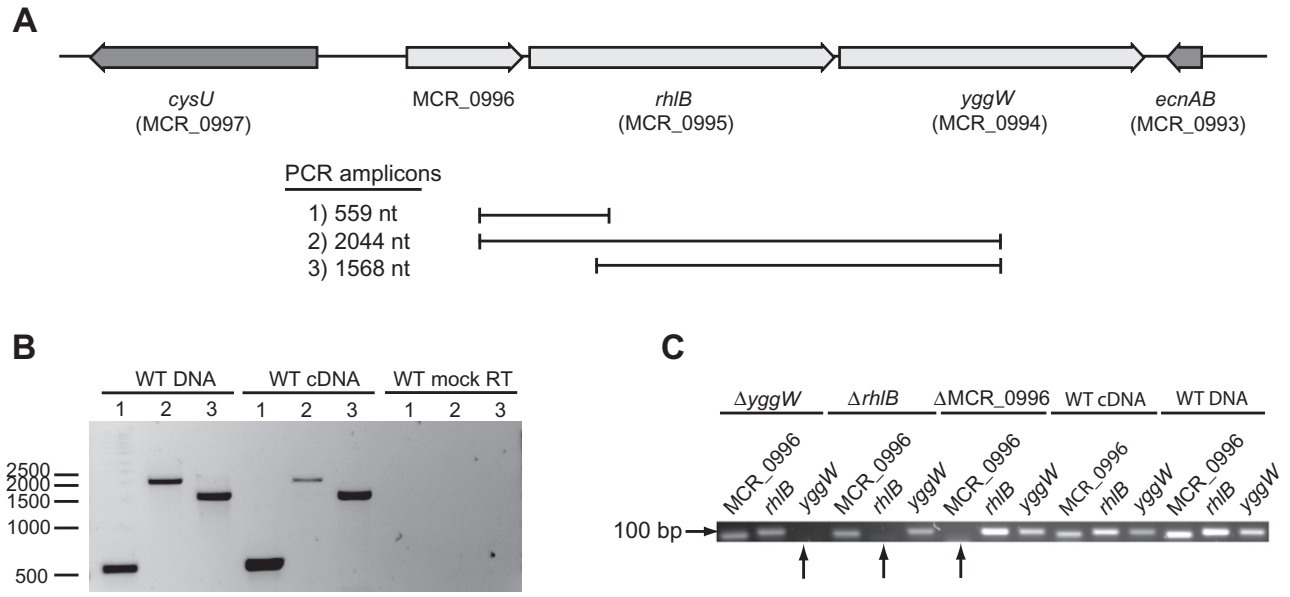


**Fig. 4.** MCR_0996-*rhlB*-*yggW* operon validation and expression analysis.
A. Chromosomal organization of the gene cluster and illustration of gene spanning PCR amplicons for operon analysis.
B. Gene spanning PCR reactions on cDNA showed that the MCR_0996-*rhlB*-*yggW* gene cluster functions as an operon. No products were observed for the mock reverse transcriptase (RT) reaction.
C. Deletion of one gene did not affect expression of other genes in operon as only expression of the deleted gene was found to be absent, indicated with arrows.

tial growth in BHI medium. Standard broth growth conditions were chosen because none of the directed mutant strains were able to grow sufficiently under iron-limiting conditions. The highest number of differentially expressed genes were due to the deletion of *yggW* and MCR_0457 (Fig. 6A), 393 and 192 genes respectively. Considerably fewer differentially expressed genes were found in Δ*rhlB* (9 genes), ΔMCR_0996 (22 genes) and Δ*rnd* (38 genes) (Fig. 6A). All genes that met the selection criteria for differential expression (see *Experimental procedures*) are listed in Table S1.

Expression of the *narGHJI* gene cluster, encoding nitrate reductase subunits, was higher in all mutants, while expression of the gene encoding nitrite reductase (AniA), which catalyses the next step of denitrification (conversion of nitrite to nitric oxide), was lower in all mutant strains. Furthermore, expression of MCR_0136, encoding a conserved hypothetical protein, was decreased in all mutant strains by 2.3- to 4.9-fold compared with wild-type. Interestingly, expression of the gene encoding the multifunctional ubiquitous surface protein A2H (UspA2H), involved in adhesion, biofilm formation and complement resistance (Riesbeck *et al.*, 2006; de Vries *et al.*, 2009), was increased 2.3- and 2.5-fold in the ΔMCR_0996 and ΔMCR_0457 strains respectively. Only a limited overlap was observed between the gene sets of the mutant strains with the highest number of differentially expressed genes, Δ*yggW* and ΔMCR_0457, which shared 20 genes that showed higher expression and 18 of which expression was reduced (Fig. 6B). These included elevated levels of *narK2*, encoding a putative nitrate/nitrite transporter and lower expression of the nitrate-binding protein gene *nrtA* of a nitrate ABC transporter.

The differentially expressed genes in the Δ*yggW* strain were distributed among a variety of functional categories (Fig. 6C and Table S2), with a significant enrichment of the 'conserved hypothetical and hypothetical proteins' class among the higher expressed genes, and enrichment of 'protein biosynthesis' genes among the genes of which expression was decreased, including 30 genes that code for the ribosomal subunits and two genes encoding translation elongation factors. In the ΔMCR_0457 strain, significant enrichment of 'transport and binding proteins' was observed in the gene set with reduced expression (Fig. 6C and Table S2).

Interestingly, in the Δ*yggW* strain there was a ~ 23-fold increase in expression of a putative bacterioferritin-associated ferredoxin (MCR_1040) that is predicted to be involved in the release of iron from the intracellular iron-storage protein bacterioferritin, as well as higher expression of the genes encoding the ferredoxins MCR_0899 and MCR_1709, glutaredoxin and glutaredoxin-like proteins (MCR_0600 and MCR_1266 respectively), AhpC/TSA family protein (MCR_1068), and the thioredoxins MCR_1740 and MCR_0506. Further, we observed lower expression of the genes coding for a rubredoxin family

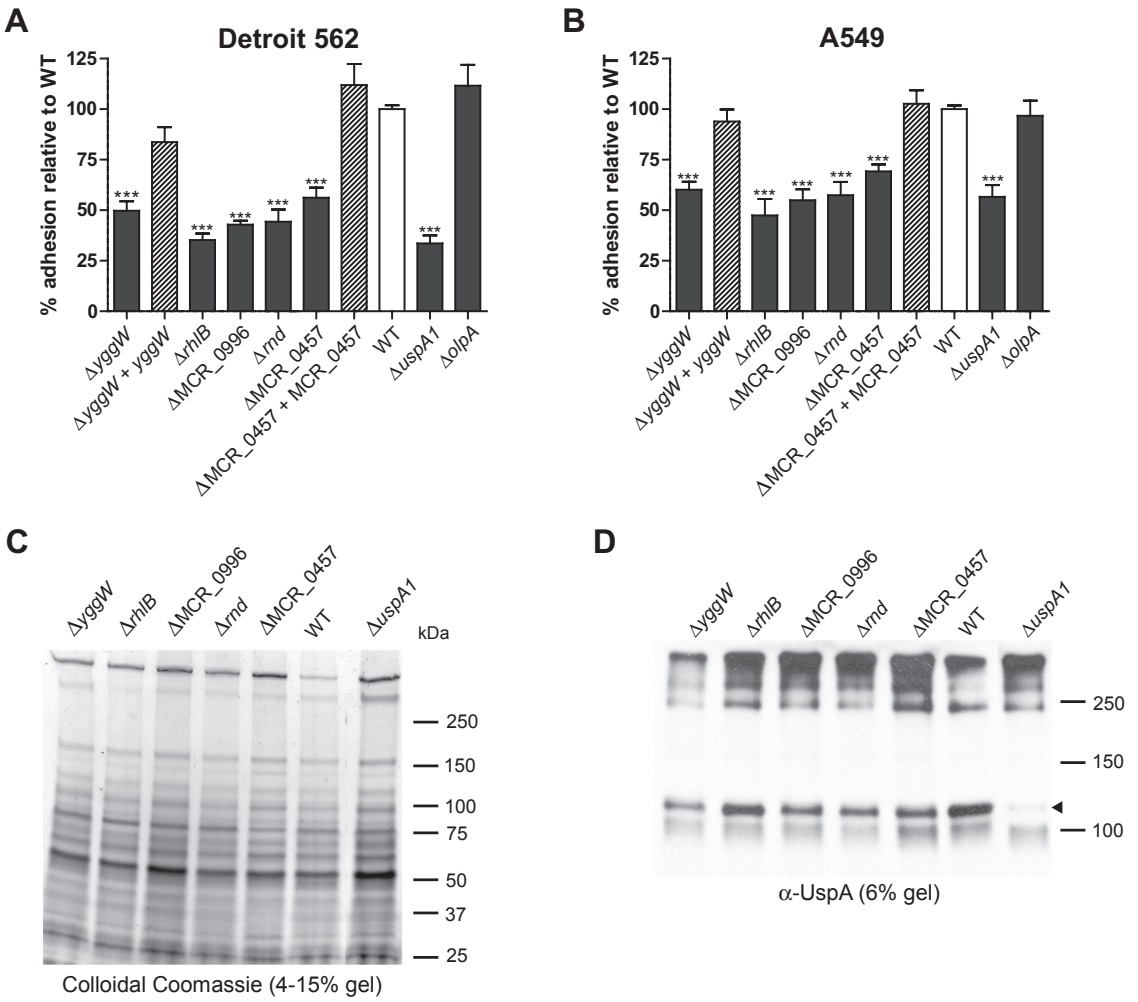


**Fig. 5.** Adhesion characteristics of mutants to respiratory tract epithelial cells, analysis of outer membrane profiles and UspA1 protein expression.
A and B. Adherence of the *yggW*, *rhlB*, MCR_0996, *rnd* and MCR_0457 mutants to Detroit 562 pharyngeal epithelial cells (A) and A549 type II alveolar epithelial cells (B) was found to be significantly attenuated as compared with the wild-type strain. Adhesion of complemented Δ*yggW* and ΔMCR_0457 was fully restored to wild-type levels. Deletion of *uspA1*, encoding the major adhesin of *M. catarrhalis*, clearly diminished adherence, whereas this was not the case upon deletion of the *olpA* gene. Adherence is expressed as percentage of wild-type (WT) ($n \geq 4$) and shown as means and SEM. Statistical difference was determined with a Mann–Whitney test with $^{***}P < 0.001$.
C. Outer membrane profiles of directed mutant strains, as analysed by SDS-PAGE and colloidal Coomassie staining, were highly similar to the pattern observed for the wild-type strain.
D. Western blot analysis showed that UspA1 expression was detected in all mutant strains. The band of ~ 115 kDa (indicated with black arrow) was lacking in the UspA1 mutant but present in the other mutant strains.

protein (MCR_0041), cytochrome *c* biogenesis proteins (MCR_1234–1235 and MCR_1321) and NADH-quinone oxidoreductase subunit H (MCR_0715). These results might reflect a changing/altered redox balance in the Δ*yggW* strain. In addition, deletion of the *yggW* gene resulted in increased expression of 15 genes encoding putative membrane proteins, as well as 120 conserved hypothetical and hypothetical proteins (46.8% of the total number of genes with increased expression).

Considerably fewer genes were found to be differentially expressed in the mutants of the two other genes of the MCR_0996-*rhlB-yggW* operon, namely *rhlB* and MCR_0996 (Fig. 6A). Among the lower expressed gene set of ΔMCR_0996 were genes encoding the iron-sulphur protein assembly chaperones HscA (MCR_0604) and HscB (MCR_0605). An example of a differentially expressed gene in the Δ*rnd* mutant is the NRAMP family Mn2+ and Fe2+ transporter gene (MCR_0789), with a 4.5-fold increase in expression.

In the ΔMCR_0457 strain, several genes belonging to the functional category 'transport and binding proteins' were lower expressed, including transporters for nitrate (MCR_0038–0040), phosphate (MCR_1732–1734), sulphate (MCR_0997–0998), zinc (MCR_0370), and the

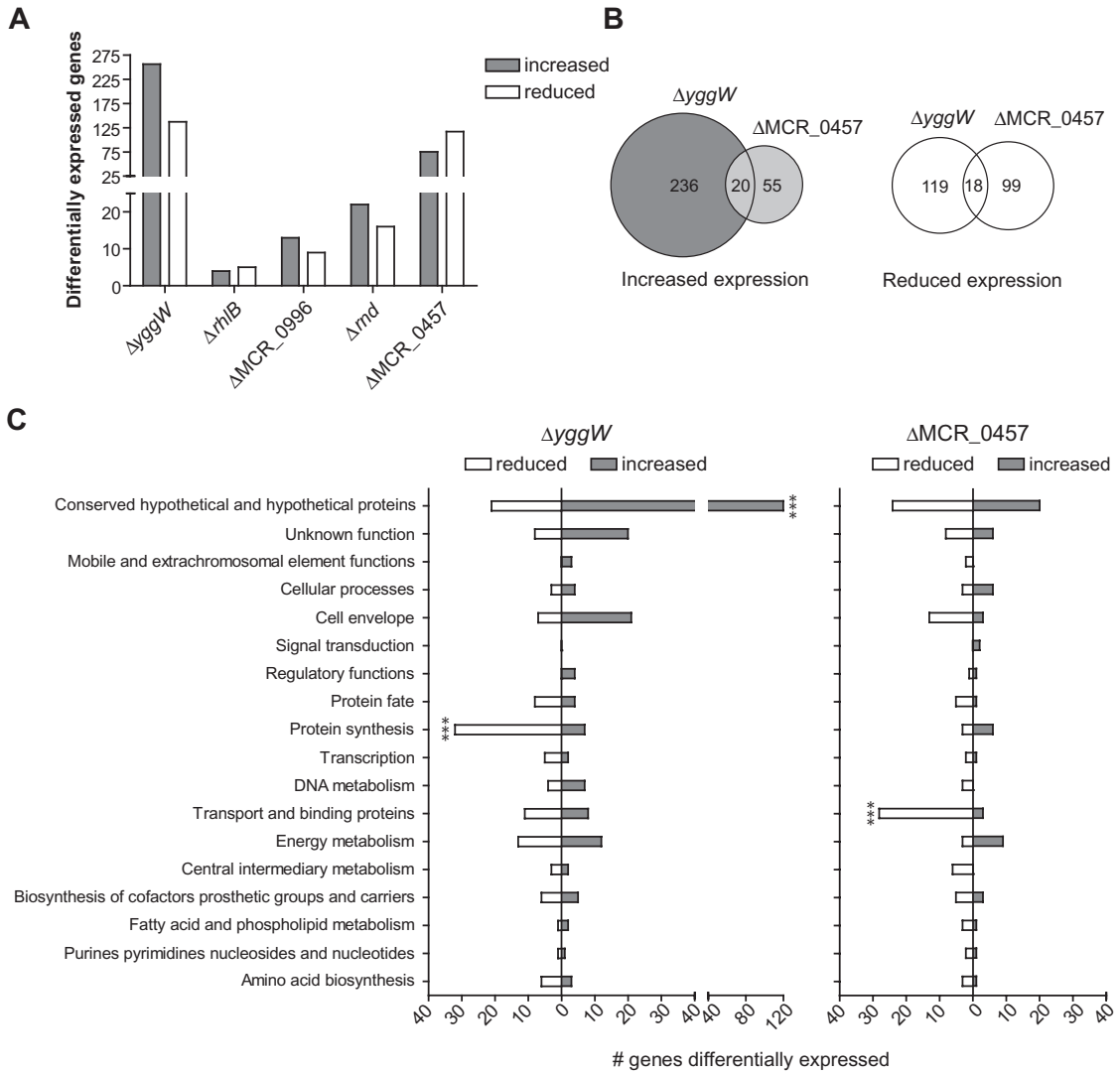


**Fig. 6.** Differentially expressed genes identified by transcriptional profiling of directed mutant strains.
A. Number of genes with increased or reduced expression per directed mutant strain ($n \geq 3$). Deletion of *yggW* and MCR_0457 resulted in a high number of differentially expressed genes, whereas considerably less genes were differentially expressed in the other mutant strains.
B. Overlap of differentially expressed genes in Δ*yggW* and ΔMCR_0457. Only a limited overlap between both mutants was observed.
C. Functional class distribution of differentially expressed genes in Δ*yggW* and ΔMCR_0457. Functional class enrichment was determined using Fishers exact test and corrected for multiple testing, ***$Q$-value < 0.001.

NRAMP family Mn2+ and Fe2+ transporter (MCR_0789), as well as the oligopeptide ABC transport system (MCR_1304–1306). Interestingly, several genes that were previously found to have increased expression under iron-limiting conditions were identified as higher expressed in this mutant, including genes encoding LbpB, TbpA, and the BadM/Rrf2 family transcriptional regulator MCR_0609 (Wang *et al.*, 2007). Finally, several genes of the haem biosynthesis pathway were differentially expressed in the ΔMCR_0457 mutant, more specifically, *hemCD* expression was higher, and expression of *cobA*, *hemF* and *hemN* was decreased.

## Discussion

Since the human host is devoid of free iron, respiratory tract pathogens like *M. catarrhalis* will encounter a period of iron starvation upon entering their host. In this study, we aimed to extend our knowledge of iron metabolism in *M. catarrhalis* by the genome-wide identification of genes essential for growth under iron-limiting conditions using an improved GAF technology. As such, this is the first high-throughput genome-wide screen to identify conditionally essential genes in *M. catarrhalis*.

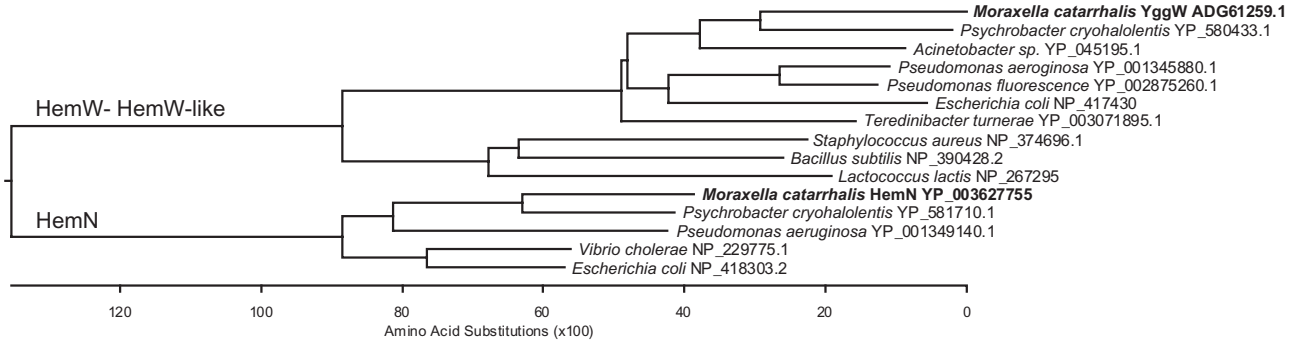


**Fig. 7.** Phylogenetic relationship analysis of the *M. catarrhalis* YggW protein. YggW belongs to the group of HemW- and HemW-like proteins as it clusters with *Psychrobacter* sp. and *Acinetobacter* sp. HemW- and HemW-like proteins. Analysis was conducted using the CLUSTALW alignment method in MegAlign (Lasergene).

By GAF we were able to identify five genes (*yggW, rhlB*, MCR_0996, *rnd* and MCR_0457) as being essential for growth of *M. catarrhalis* BBH18 under iron-limiting conditions. The importance of these five genes during iron starvation was confirmed using directed mutants and attenuated growth could be restored upon iron repletion. Even though we analysed close to the whole BBH18 genome by screening of a ~ 28 000 mariner transposon mutant library, the number of individual attenuated transposon mutants (eight transposon insertion mutants corresponding to five genes) was rather low, which could indicate a relatively high rate of false negatives. There are several factors that may have influenced the number of identified attenuated transposon mutants. First, our GAF microarrays do not allow identification of all transposon insertion sites, as the cDNA probes of more than one transposon mutant can contribute to the signal of individual array probes (spaced every 200 bp). Furthermore, our experimental set-up was aimed at reducing the number of false-positives rather than avoiding false-negatives, as we combined sufficient biological variation between replicates with stringent selection criteria during data analysis. We did not identify any of the known iron-acquisition factors such as CopB and LbpA/B in our screen, presumably due to the high redundancy in iron acquisition and transport mechanisms, underscored by our observation that the growth rate of Δ*copB* and Δ*lbpA* under iron-limiting conditions did not differ from the wild-type strain.

A shared characteristic between all the mutant strains was the increased expression of genes encoding the nitrate reductase subunits, which may point towards a non-functional aerobic respiration or to low oxygen tension. Importantly, expression of *aniA*, responsible for the next step in denitrification, was decreased in all mutants, probably resulting in the accumulation of nitrite. In Δ*yggW* and ΔMCR_0457 this may be counteracted by the decreased *narK2* levels, encoding a putative nitrate/nitrite transporter. Further, a large number of conserved hypothetical and hypothetical proteins was differentially expressed, especially in Δ*yggW*. As pointed out by Galperin and Koonin (2010), many of the highly conserved hypothetical proteins are typically associated with processes such as translation, transcription or ribosome biosynthesis, whereas hypothetical genes with less conservation may be involved in cellular maintenance processes that deal with waste products generated during various cellular and metabolic processes. This might be particularly important for aerobic organisms that have to cope with spontaneous oxidation of nucleotides, amino acids, lipids and other cellular components.

The *yggW* mutant showed the most prominent growth defect under iron-limiting conditions, which was restored to near wild-type levels by genetic complementation. Deletion of *yggW* in three other *M. catarrhalis* isolates resulted in similar attenuated phenotypes, indicating a conserved role in *M. catarrhalis*. Based on homology, *yggW* is predicted to encode for an oxygen-independent coproporphyrinogen-III oxidase-like protein, catalysing the oxidative decarboxylation of coproporphyrinogen-III to protoporphyrinogen, but experimental evidence that YggW or homologous proteins can catalyse this enzymatic conversion is lacking. *M. catarrhalis* YggW shares low levels of amino acid identity with HemN (23.9%) and HemF (9.6%) proteins, which are reported to catalyse this oxidative decarboxylation reaction (Layer *et al*., 2010), providing indirect evidence that YggW fulfils another function. Recently, it was reported that *Lactococcus lactis hemN* was incorrectly annotated as an oxygen-independent coproporphyrinogen-III dehydrogenase (CPDH) as the purified protein was devoid of CPDH activity (Abicht *et al*., 2011). The gene was re-annotated as *hemW* and functional characterization showed that *L. lactis* HemW plays a role in haem trafficking. Phylogenetic analysis clearly showed that *M. catarrhalis* YggW, as well as homologues in other closely related species such as *Psychrobacter* sp. and *Acinetobacter* sp., group into the cluster of HemW- and

HemW-like proteins, especially those of Gram-negative origin (Fig. 7). Further proof that *M. catarrhalis* YggW belongs to this family can be found in HemW-specific sequence domains and motifs (Abicht *et al*., 2011). As all HemW family proteins, *M. catarrhalis* YggW harbours the iron-sulphur cluster CxxxCxxC motif, whereas HemN proteins possess the radical SAM enzyme motif CxxxCxx-CxC with four cysteine residues, which is also present in *M. catarrhalis* HemN. In addition, the HemW conserved HNxxYW motif is also present in *M. catarrhalis* YggW. Haem is involved in various processes ranging from respiration to oxidative stress responses, being a cofactor of cytochromes and catalase respectively. The transcriptome of Δ*yggW* suggested a changing or altered redox balance, which may be the result of an improper functioning of the cytochromes in the respiratory chain due to a reduced haem loading of cytochromes. We could not identify a potential link between YggW function and the oxidative stress response, as the sensitivity for several chemical oxidants was not affected by the deletion of *yggW*. Therefore, the YggW protein is expected to be involved in the shuttling of haem from the cytoplasm to the periplasm or vice versa. We speculate that YggW is involved in haem loading of cytochromes.

YggW was shown to be part of an operon, of which the other two genes, MCR_0996 and *rhlB*, were also picked up in our GAF screen. However, based on their annotation, no obvious functional connection between the genes that comprise the MCR_0996-*rhlB*-*yggW* operon exists. In line with this, no relationship between these genes in other species could be found using the Search Tool for the Retrieval of Interacting Genes (STRING) (Szklarczyk *et al*., 2011) (data not shown). The potential function of the hypothetical MCR_0996 remains as yet unknown, as no functional homologues in other species exist, and it does not possess any known conserved domains. The *rhlB* gene, like *rnd*, the fourth identified gene, may potentially play a role in the adaptation to changing environmental conditions. The RhlB protein is part of the multicomponent complex called the degradosome, which is involved in the degradation of RNAs (Arraiano *et al*., 2010). RND is one of many ribonucleases present in the *M. catarrhalis* BBH18 genome. In *Escherichia coli* RND is involved in the 3′ maturation of several stable RNAs including 5S rRNA, tRNA, but also small structured RNAs (Li *et al*., 1998). In this light, RND could intervene in the translation of mRNA into proteins. RND requires divalent metal ions to fulfil its function; however, it remains unclear which ion is required for *M. catarrhalis* RND activity. The combined effect of regulation of tRNA, rRNA availability and RNA decay likely enables the bacterium to adapt to the iron-limiting conditions that are also faced at the host mucosa. The transcriptional profiles of the Δ*rhlB* and Δ*rnd* mutants were very similar to the wild-type strain, but our microarrays did not provide for analysis of small RNAs, which may be altered in these mutant strains.

The fifth identified gene was MCR_0457, encoding a hypothetical protein. The role of MCR_0457 in growth under iron-limiting conditions was confirmed by genetic complementation, but appeared to be specific for strain BBH18. BLAST analysis only revealed low level identity (23–37%) homologues of MCR_0457 in *Enhydrobacter* sp., *Psychrobacter* sp. and *Acinetobacter* sp., and no functional domains were detected. However, we did find a potential link with haem metabolism, as MCR_0457 resides in a putative operon with MCR_0456, encoding a delta-aminolevulinic acid dehydratase (porphobilinogen synthase, HemB), which is involved in haem biosynthesis. Interestingly, some of the differentially expressed genes in this mutant are also known to be differentially expressed under iron-limiting conditions including *lbpA, tbpA*, and the gene encoding the BadM/Rrf2 family transcriptional regulator, which also showed increased expression in a Chinchilla colonization model (Wang *et al*., 2007; Hoopman *et al*., 2012).

For any pathogen, successful colonization and infection of the respiratory tract mucosa depends on its ability to adhere to the epithelial cell layer as well as to acquire essential nutrients such as iron. As iron is an important cofactor in various cellular and metabolic processes, changes in iron metabolism may reduce virulence and/or bacterial fitness. For example, studies in *Bordetella pertussis* showed that iron starvation resulted in increased adherence to respiratory tract epithelial cells by enhancing mucin binding (Vidakovics *et al*., 2007). In *Neisseria meningitidis*, deletion of *znuD*, involved in haem utilization, resulted in reduced adherence to A549 type II alveolar cells (Kumar *et al*., 2012). In this study, we observed that the *M. catarrhalis* mutants attenuated for growth under iron-limiting conditions, were also attenuated for adherence to both A549 type II alveolar and Detroit 562 pharyngeal epithelial cells. Importantly, gene expression of the known *M. catarrhalis* adhesion factors such as UspA1 (also confirmed on protein level by Western blot), *M. catarrhalis* adherence protein (McaP) or *Moraxella* IgD-binding protein (MID/Hag) was not changed in the mutant strains. In line with this, Wang *et al*. showed that exposure of *M. catarrhalis* to iron-limiting conditions did not affect gene expression of UspA1 or MID/Hag (Wang *et al*., 2007), which may suggest that restricted iron availability influences the physiology or fitness of the bacterium in a more general way.

In conclusion, we describe the successful use of the adapted GAF technology for high-throughput identification of genes required for *M. catarrhalis* growth/survival during iron starvation. Future application of this technology to various *in vivo* relevant conditions will increase our understanding of *M. catarrhalis* pathogenesis.

## Experimental procedures

### *Bacterial strains, growth conditions and plasmids*

All strains and plasmids are summarized in Table S3. *M. catarrhalis* strains were routinely cultured on brain–heart infusion (BHI) agar plates at 37°C in an atmosphere containing 5% $CO_2$ or in BHI broth at 37°C at 200–250 r.p.m. Transposon mutant libraries, gene deletion mutants and genetically complemented strains were cultured in BHI in the presence of 30 μg $ml^{-1}$ spectinomycin (BHI-spec) and/or 15 μg $ml^{-1}$ kanamycin. Naturally competent *M. catarrhalis* bacteria were obtained by growing cultures until early log-phase ($OD_{620}$ ~ 0.2–0.3). Aliquots of bacteria were routinely stored in the presence of 20% glycerol at –80°C. The *marinerT7* transposon from pR412T7 (Akerley *et al*., 1998) was amplified with a single phosphorylated primer PBGSF20 and cloned into the pCR2.1 vector (Invitrogen) to obtain pGSF8. For genetic complementation of directed mutants, the spectinomycin resistance cassette of pWW115 (Wang and Hansen, 2006) was replaced a kanamycin resistance cassette as follows. The kanamycin resistance cassette was amplified from pR410 (Burghout *et al*., 2007) and subcloned in pGEMT-easy (Promega). Via restriction digestion, the kanamycin resistance cassette was ligated into the PciI and BsrGI sites of pWW115 downstream of the spectinomycin resistance cassette promoter, resulting in pSV001.

### *Construction of* M. catarrhalis *transposon mutant libraries*

A large random mariner transposon mutant library was generated in *M. catarrhalis* BBH18 essentially as described previously (Bijlsma *et al*., 2007; Burghout *et al*., 2007). For *in vitro* transposon mutagenesis, 10 μg of BBH18 chromosomal DNA (Qiagen Genomic-tip 20/G isolated) was incubated with 5 μg of pGSF8 and 10 μg of purified HinmarC9 transposase in a 200 μl reaction volume. After repair of the transposition reaction, 1 ml of naturally competent BBH18 bacteria was transformed with 100 μl of mutagenized DNA in a total volume of 5 ml (adjusted with BHI medium). After a 3 h incubation at 37°C and 200 r.p.m., transformants were selected on BHI-spec plates. Subsequently, 28 000 independent transformants were scraped from the plates, pooled, expanded to an $OD_{620}$ ~ 0.6 and stored at –80°C.

### *GAF screen under iron-limiting conditions*

The *marinerT7* mutant library was pre-cultured to mid-log phase ($OD_{620}$ ~ 1.0), washed in 2 volumes of PBS supplemented with 0.15% gelatin (PBS-G) and resuspended in 0.5 volume PBS-G. This suspension was used to inoculate either BHI-spec medium that was pre-treated overnight with 30 μM Desferal (Sigma Aldrich) (challenge condition, BHI-DF30) or untreated BHI-spec medium (control condition, BHI-DF0) to an $OD_{620}$ ~ 0.1. At the mid-log and early-stationary-phase mutants were recovered from the cultures and stored at –80°C. This experiment was performed four times (two times on two different days). The recovered mutants were expanded for chromosomal DNA isolation using Genomic-tip 20/G columns. Next, 4 μg of DNA was digested with 30 U of AluI restriction enzyme (New England Biolabs). Digestions were assessed for completion on a 1% agarose gel and purified using the MinElute reaction clean-up kit (Qiagen). Two micrograms of digested DNA served as a template for a T7 RNA polymerase reaction (T7 MegaScript kit, Ambion) using the outward-facing T7 sites of the transposon element. This resulted in the generation of mutant-specific T7 RNA fragments that flank both sides of the transposon insertion. The template DNA was degraded with DNase I and the T7 RNA was purified using the RNeasy Minelute kit (Qiagen). Two micrograms of T7 RNA was reverse transcribed into cDNA in the presence of 16.7 ng $\mu l^{-1}$ actinomycin D (ActD, Sigma Aldrich) using 1 μg of Cy3-labelled random nonamers (Nimblegen) for priming, essentially as described in de Vries *et al.* (2010). Through the addition of ActD, formation of double-stranded cDNA is inhibited (Perocchi *et al*., 2007), ensuring strand-specific cDNA synthesis and thus asymmetrical generation of mutant-specific cDNA probes. The obtained Cy3-labelled mutant-specific cDNA was purified using CyScribe columns (GE healthcare Life Sciences), concentrated using YM-30 columns (Millipore) and subsequently used for hybridization to custom-designed Nimblegen microarrays.

### *GAF microarray analysis*

The custom-designed Nimblegen 4 × 72 K GAF microarray design was based on the AluI-restriction fragments of the *M. catarrhalis* BBH18 genome (de Vries *et al*., 2010). Nimblegen probes (50–72 nt) were designed on the 3′ and 5′ ends of all AluI fragments > 70 nucleotides (nt) and in case of fragments > 400 bp, spaced every ~ 200 bp on both strands. This allowed mapping of the transposon insertion with a ~ 200 bp resolution. Of the 6085 AluI fragments larger than 70 nt, probes could be designed for 6003 fragments, resulting in a total of 20 078 experimental probes. In addition to three replicates of each experimental probe, the array contained 11 803 negative-control probes with a length distribution and G+C content similar to those of the experimental control probes. Two micrograms of Cy3-labelled mutant-specific cDNA was hybridized to the GAF microarrays overnight at 42°C using a Nimblegen hybridization station according to the manufacturer's instructions. After washing, raw images were obtained using the MS200 microarray scanner (Nimblegen) and processed using NimbleScan software. ANAIS (Simon and Biot, 2010) was used for intra-array (background adjustment) and inter-array (quantile) normalization to obtain normalized probe signal intensities (SI). Normalized probe SI were corrected for a threshold of five times the median SI of the negative-control probes. Statistical analysis was performed on the ratio between the SI of the control and challenge (iron-limiting) conditions using the CyberT implementation of Student's *t*-test (cybert.microarray.ics.uci.edu). The false discovery rate (FDR) was calculated from the $P_{bayes}$ as described in van Hijum *et al.* (2005). Final selection criteria consisted of a fold-change > 1.9 (control/challenge), a $P_{bayes} < 0.001$ and a FDR < 0.01.

### *Generation of directed mutants*

Directed gene deletion mutants of *M. catarrhalis* BBH18 were generated by allelic exchange of the target gene with a spec-

tinomycin resistance cassette, essentially as described in Burghout *et al*. (2007). In short, an extension PCR was performed to join 400–500 bp 5′ and 3′ flanking sequences of a target gene with the spectinomycin resistance cassette (obtained from pR412T7), which was subsequently transformed into naturally competent *M. catarrhalis* BBH18 bacteria. For this, 10 μl of PCR product was mixed with 100 μl competent cells and 400 μl of BHI medium, incubated for 3–5 h at 37°C and 200 r.p.m., and transformants were selected on BHI-spec plates. Transformants were checked by PCR for recombination at the desired location on the chromosome. Next, 0.5–1 μg of DNA of the first-generation directed mutants was crossed back into the BBH18 wild-type strain and selected on BHI-spec plates. At the same time, competent cells were also processed through the transformation procedure to obtain a coupled wild-type strain. Gene deletions of *yggW* and MCR_0457 in strains O35E, 7169 and 46P47B1 were generated by transformation of a PCR product amplified from the corresponding BBH18 mutants containing the spectinomycin resistance cassette and gene flanking regions. All primers used in this study (obtained from Biolegio, Nijmegen, the Netherlands) are shown in Table S4.

### *Genetic complementation of yggW and MCR_0457 directed mutants*

For genetic complementation of the BBH18 *yggW* mutant, PCR products of the *yggW*-coding sequence (CDS) and the *bro-1* promoter of strain BC7 (Davie *et al*., 2011) were joined via an overlap PCR. To this end, the reverse *bro-1* promoter primer contained an overhang complementary to the forward *yggW* amplicon primer. The joined *bro-1* promoter-*yggW* sequence was ligated into the XmaI and SacI sites of pSV001. To complement ΔMCR_0457, the CDS and upstream region was amplified from BBH18 and ligated into the BamHI and SacI sites of pSV001. For restriction digestions, amplicons were first subcloned into pGEMT-easy (Promega). To obtain the complemented mutants, plasmid ligation mixtures were first transformed into Δ*yggW* and ΔMCR_0457 of *M. catarrhalis* O35E as this strain is more easily transformable than BBH18. Subsequently, plasmid DNA was isolated from resulting O35E transformants and used to transform BBH18 mutants and wild-type strains.

### In vitro *growth under iron-limiting and iron-repleted conditions*

The directed mutants and their parental wild-type strains were expanded to mid-log phase, washed in 2 volumes PBS-G, and resuspended in PBS-G to an $OD_{620}$ of 1.0. From this suspension, 200 μl was used to inoculate either overnight DF30 pre-treated BHI or untreated BHI. Colony-forming units (cfu) were determined at 0, 2, 4 and 5.5 h of growth by plating 10-fold serial dilutions. For GAF validation and chemical complementation experiments with *M. catarrhalis* BBH18 mutants and wild-type strains, growth speed of the directed mutants was calculated between the 2 and 5.5 h time point as follows: *n* (number of generations) = 3.3 (log cfu at 5.5 h time point – log cfu at 2 h time point), generation time g (hours) = *n*/2.5 h, growth rate constant K (generations per hour) = ln 2 $g^{-1}$. For chemical complementation, DF30-treated medium was supplemented with iron sulphate (Sigma Aldrich) or bovine haemin (Sigma Aldrich) to a final concentration of 100 μM and 20 μM respectively. For GAF validation experiments ($n \geq 3$) with BBH18 mutants and wild-type strains, statistical difference was determined with a Mann–Whitney test. Statistical analysis of chemical complementation experiments ($n = 2$) was performed with unpaired *t*-test with Welch's correction. Growth experiments with genetically complemented *yggW* and MCR_0457 BBH18 mutant strains ($n \geq 5$) were conducted in BHI pre-treated with DF30. The statistical differences were determined on $\log_{10}$-transformed data with a two-way ANOVA and a Bonferroni *post hoc* test. Growth of O35E, 7169 and 46P47B1 ($n \geq 4$) mutant strains under iron-limiting conditions were conducted at 30 μM and 20 μM (DF20). Statistical analysis were performed on $\log_{10}$-transformed data with a two-way ANOVA and a Bonferroni *post hoc* test.

### *MCR_0996-rhlB-yggW operon validation and expression analysis*

Cultures of directed mutants (Δ*yggW*, Δ*rhlB*, ΔMCR_0996) and their parental wild-type strain were grown in BHI to an $OD_{620}$ of ~ 1.0 and RNA was isolated as described in de Vries *et al*. (2010). cDNA was generated using the Superscript III reverse transcriptase kit (Qiagen) by using gene-specific primers for operon analysis and random hexamers for the single gene expression analysis. Amplifications were performed using the AmpliTaq system (Sigma Aldrich) and analysed on 1% and 2% agarose gels respectively.

### *Adhesion of directed mutants to respiratory tract epithelial cells*

The human pharyngeal epithelial cell line Detroit 562 (ATCC CCL-138) and the type II alveolar epithelial cell line A549 (ATCC CCL-185) were routinely grown in DMEM with GlutaMAX™-I and 10% fetal calf serum (FCS) (Invitrogen) at 37°C and 5% $CO_2$. Two days prior to the adherence assay, $2{\cdot}10^5$ Detroit 562 cells per well were seeded into a 24-well tissue culture plate, and after 1 day, the growth medium was refreshed. A549 cells were seeded into 24-well tissue culture plates one day prior to the assay at $4{\cdot}10^5$ cells. For both cell lines, monolayers of approximately $1{\cdot}10^6$ cells per well were used for adherence assays. *M. catarrhalis* BBH18 wild-type and mutant strains were cultured under standard growth conditions (BHI medium, iron-rich) until mid-log phase ($OD_{620}$ ~ 1.0) and stored at –80°C. The bacteria were washed once in DMEM with GlutaMAX™-I and 1% FCS (infection medium) and resuspended in the infection medium to $1{\cdot}10^7$ cfu $ml^{-1}$. Epithelial cells were washed twice with PBS, infected with 1 ml of the *M. catarrhalis* suspension (multiplicity of infection, 10 bacteria per cell), centrifuged for 5 min at 200 *g*, and incubated 1 h at 37°C in a 5% $CO_2$ environment. Non-adherent bacteria were removed by three washes with PBS, after which 1 ml of 1% saponin (Sigma Aldrich) in PBS-G was added to detach and lyse the Detroit or A549 cells. Colony-forming units were enumerated by plating 10-fold serial dilutions on BHI plates supplemented with the appropriate antibiotics. The percentage adherence of the mutants was

expressed relative to the percentage adherence of the wild-type. Each experiment was performed at least four times and statistical difference was determined with a Mann–Whitney test.

### *Analysis of outer membrane protein profiles and UspA1 expression*

Wild-type and mutant strains were cultured till $OD_{620}$ of 1.0–1.2 and harvested by centrifugation. Outer membranes were isolated using the ReadyPrep Membrane I kit (Bio-Rad) accordance to manufacturer's instructions. During the lysis procedure, glass beads were added for homogenization with the TissueLyser LT (Qiagen). Protein quantification was performed using the 2D-Quant Kit (GE Healtcare). Five micrograms of outer membrane preparations were separated on a 4–15% TGX gel (Bio-Rad) and analysed by colloidal Coomassie staining (Pink *et al*., 2010). To analyse UspA1 protein expression, 5 μg was separated on a 6% SDS-page gel and blotted on PVDF membranes. Blots were blocked overnight in blocking buffer [1% BSA and 2% skimmed milk powder in PBS with 0.1% tween20 (PBS-T)]. Polyclonal anti-UspA1/A2 rabbit serum was diluted 1:500 in blocking buffer and incubated for 2 h at room temperature. Blots were washed three times in PBS-T and incubated with swine anti-rabbit conjugated with horseradish peroxidase (Dako) for 1 h. Proteins were detected with ECL plus reagent (GE healthcare).

### *RT-qPCR expression analysis*

Strains were expanded to $OD_{620}$ ~ 1.0 ($n = 3$) and RNA was isolated as previously described (de Vries *et al*., 2010). DNA-free total RNA (500 ng) was reverse transcribed into cDNA with random primers (300 ng) using the Superscript III kit (Invitrogen). Expression of *yggW* and MCR_0457 in mutants or complemented mutants was determined relative to wild-type with the ΔΔCt method (Livak and Schmittgen, 2001). RT-qPCR reactions were performed using SYBR green chemistry on a 7500 Fast real-time PCR machine (Applied Biosystems). The *rpoD* gene was included as a reference gene for data normalization.

### *Gene expression profiling of directed mutants*

*Moraxella catarrhalis* BBH18 directed mutants ($n = 3$) and their parental wild-type BBH18 strain ($n = 4$) were expanded to mid-log phase ($OD_{620}$, 1.2–1.4) and RNA was isolated as previously described (de Vries *et al*., 2010). Total RNA (5 μg) was labelled according to standard Nimblegen gene expression array protocols. The Nimblegen *M. catarrhalis* BBH18 expression array contained eight probes per CDS, with each probe represented four times, and 7298 negative control probes. CDS represented on the array included all ORFs predicted in BBH18 (de Vries *et al*., 2010), as well as unique CDS predicted using ZCURVE (Guo *et al*., 2003), Prodigal (Hyatt *et al*., 2010), Glimmer (Delcher *et al*., 1999) or GeneMarkHMM (Lukashin and Borodovsky, 1998), sequences are available upon request. Normalization and threshold correction were performed as described for the *M. catarrhalis* GAF arrays, with the exception that the normalized probe SI were corrected for a threshold of seven times the median SI of the negative-control probes. Statistical analysis was performed on the median SI of the eight probes representing a single CDS. Genes were considered to be differentially expressed at a fold-change > 2 or < –2, $P_{bayes} < 0.0001$, FDR < 0.0001, and with the additional criteria that at least six out of eight probes met the fold-change cut-off, $P_{bayes} < 0.001$ and FDR < 0.001. Genes were also excluded if the expression was low (SI < 500) in both the wild-type and the mutant strain. Functional class distribution was assessed using the Institute for Genomic Sciences (IGS) classification (de Vries *et al*., 2010). Functional class enrichment was assessed using the Fishers exact (one-tail) test, corrected for multiple testing per directed mutant strain according to Storey and Tibshirani (2003).

### *Microarray data*

All microarray data have been deposited in NCBI Gene Expression Omnibus (GEO) database (http://www.ncbi.nlm.nih.gov/geo/) under GEO Series Accession No. GSE41548, subseries GSE41546 for GAF microarrays and subseries GSE41547 for expression profiling data.

### *Statistical analysis*

Statistical analyses were performed in GraphPad Prism 5.0 (GraphPad Software) unless indicated otherwise, with $P < 0.05$ considered to be significant.

## Acknowledgements

This study was financially supported by Vienna Spot of Excellence (VSOE) grant (ID337956). We thank Marc Eleveld and Rob Rademakers for technical assistance. We are grateful to Eric Hansen for sharing the pWW115 plasmid and to Kristian Riesbeck for sharing the UspA1/A2 antibody. Further, we thank Garth Ehrlich for kindly providing the O35E, 7169 and 46P47B1 strains.

## References

Abicht, H.K., Martinez, J., Layer, G., Jahn, D., and Solioz, M. (2011) *Lactococcus lactis* HemW (HemN) is a heme-binding protein with a putative role in heme trafficking. *Biochem J* **442:** 335–343.

Aebi, C., Stone, B., Beucher, M., Cope, L.D., Maciver, I., Thomas, S.E., *et al*. (1996) Expression of the CopB outer membrane protein by *Moraxella catarrhalis* is regulated by iron and affects iron acquisition from transferrin and lactoferrin. *Infect Immun* **64:** 2024–2030.

Aebi, C., Lafontaine, E.R., Cope, L.D., Latimer, J.L., Lumbley, S.L., McCracken, G.H., and Hansen, E.J. (1998) Phenotypic effect of isogenic *uspA1* and *uspA2* mutations on *Moraxella catarrhalis* 035E. *Infect Immun* **66:** 3113–3119.

Akerley, B.J., Rubin, E.J., Camilli, A., Lampe, D.J., Robertson, H.M., and Mekalanos, J.J. (1998) Systematic identifi-

cation of essential genes by *in vitro* mariner mutagenesis. *Proc Natl Acad Sci USA* **95:** 8927–8932.

Arraiano, C.M., Andrade, J.M., Domingues, S., Guinote, I.B., Malecki, M., Matos, R.G., *et al*. (2010) The critical role of RNA processing and degradation in the control of gene expression. *FEMS Microbiol Rev* **34:** 883–923.

Bijlsma, J.J., Burghout, P., Kloosterman, T.G., Bootsma, H.J., de Jong, A., Hermans, P.W., and Kuipers, O.P. (2007) Development of genomic array footprinting for identification of conditionally essential genes in *Streptococcus pneumoniae*. *Appl Environ Microbiol* **73:** 1514–1524.

Brooks, M.J., Laurence, C.A., Hansen, E.J., and Gray-Owen, S.D. (2007) Characterization of the *Moraxella catarrhalis* opa-like protein, OlpA, reveals a phylogenetically conserved family of outer membrane proteins. *J Bacteriol* **189:** 76–82.

Burghout, P., Bootsma, H.J., Kloosterman, T.G., Bijlsma, J.J., de Jongh, C.E., Kuipers, O.P., and Hermans, P.W. (2007) Search for genes essential for pneumococcal transformation: the RadA DNA repair protein plays a role in genomic recombination of donor DNA. *J Bacteriol* **189:** 6540–6550.

Davie, J.J., Earl, J., de Vries, S.P., Ahmed, A., Hu, F.Z., Bootsma, H.J., *et al*. (2011) Comparative analysis and supragenome modeling of twelve *Moraxella catarrhalis* clinical isolates. *BMC Genomics* **12:** 70.

Delcher, A.L., Harmon, D., Kasif, S., White, O., and Salzberg, S.L. (1999) Improved microbial gene identification with GLIMMER. *Nucleic Acids Res* **27:** 4636–4641.

Du, R.P., Wang, Q., Yang, Y.P., Schryvers, A.B., Chong, P., Klein, M.H., and Loosmore, S.M. (1998) Cloning and expression of the *Moraxella catarrhalis* lactoferrin receptor genes. *Infect Immun* **66:** 3656–3665.

Galperin, M.Y., and Koonin, E.V. (2010) From complete genome sequence to 'complete' understanding? *Trends Biotechnol* **28:** 398–406.

Guo, F.B., Ou, H.Y., and Zhang, C.T. (2003) ZCURVE: a new system for recognizing protein-coding genes in bacterial and archaeal genomes. *Nucleic Acids Res* **31:** 1780–1789.

van Hijum, S.A., de Jong, A., Baerends, R.J., Karsens, H.A., Kramer, N.E., Larsen, R., *et al*. (2005) A generally applicable validation scheme for the assessment of factors involved in reproducibility and quality of DNA-microarray data. *BMC Genomics* **6:** 77.

Hoopman, T.C., Liu, W., Joslin, S.N., Pybus, C., Brautigam, C.A., and Hansen, E.J. (2011) Identification of gene products involved in the oxidative stress response of *Moraxella catarrhalis*. *Infect Immun* **79:** 745–755.

Hoopman, T.C., Liu, W., Joslin, S.N., Pybus, C., Sedillo, J.L., Labandeira-Rey, M., *et al*. (2012) Use of the chinchilla model for nasopharyngeal colonization to study gene expression by *Moraxella catarrhalis*. *Infect Immun* **80:** 982–995.

Hyatt, D., Chen, G.L., Locascio, P.F., Land, M.L., Larimer, F.W., and Hauser, L.J. (2010) Prodigal: prokaryotic gene recognition and translation initiation site identification. *BMC Bioinformatics* **11:** 119.

Kumar, P., Sannigrahi, S., and Tzeng, Y.L. (2012) The *Neisseria meningitidis* ZnuD zinc receptor contributes to interactions with epithelial cells and supports heme utilization when expressed in *Escherichia coli*. *Infect Immun* **80:** 657–667.

Layer, G., Reichelt, J., Jahn, D., and Heinz, D.W. (2010) Structure and function of enzymes in heme biosynthesis. *Protein Sci* **19:** 1137–1161.

Li, Z., Pandit, S., and Deutscher, M.P. (1998) 3′ exoribonucleolytic trimming is a common feature of the maturation of small, stable RNAs in *Escherichia coli*. *Proc Natl Acad Sci USA* **95:** 2856–2861.

Livak, K.J., and Schmittgen, T.D. (2001) Analysis of relative gene expression data using real-time quantitative PCR and the 2(−Delta Delta C(T)) method. *Methods* **25:** 402–408.

Lukashin, A.V., and Borodovsky, M. (1998) GeneMark.hmm: new solutions for gene finding. *Nucleic Acids Res* **26:** 1107–1115.

Molzen, T.E., Burghout, P., Bootsma, H.J., Brandt, C.T., van der Gaast-de Jongh, C.E., Eleveld, M.J., *et al*. (2011) Genome-wide identification of *Streptococcus pneumoniae* genes essential for bacterial replication during experimental meningitis. *Infect Immun* **79:** 288–297.

Pearson, M.M., and Hansen, E.J. (2007) Identification of gene products involved in biofilm production by *Moraxella catarrhalis* ETSU-9 *in vitro*. *Infect Immun* **75:** 4316–4325.

Pearson, M.M., Laurence, C.A., Guinn, S.E., and Hansen, E.J. (2006) Biofilm formation by *Moraxella catarrhalis in vitro*: roles of the UspA1 adhesin and the Hag hemagglutinin. *Infect Immun* **74:** 1588–1596.

Perez Vidakovics, M.L., and Riesbeck, K. (2009) Virulence mechanisms of *Moraxella* in the pathogenesis of infection. *Curr Opin Infect Dis* **22:** 279–285.

Perocchi, F., Xu, Z., Clauder-Munster, S., and Steinmetz, L.M. (2007) Antisense artifacts in transcriptome microarray experiments are resolved by actinomycin D. *Nucleic Acids Res* **35:** e128.

Pink, M., Verma, N., Rettenmeier, A.W., and Schmitz-Spanke, S. (2010) CBB staining protocol with higher sensitivity and mass spectrometric compatibility. *Electrophoresis* **31:** 593–598.

Ratledge, C., and Dover, L.G. (2000) Iron metabolism in pathogenic bacteria. *Annu Rev Microbiol* **54:** 881–941.

Riesbeck, K., Tan, T.T., and Forsgren, A. (2006) MID and UspA1/A2 of the human respiratory pathogen *Moraxella catarrhalis*, and interactions with the human host as basis for vaccine development. *Acta Biochim Pol* **53:** 445–456.

Sethi, S., and Murphy, T.F. (2008) Infection in the pathogenesis and course of chronic obstructive pulmonary disease. *N Engl J Med* **359:** 2355–2365.

Simon, A., and Biot, E. (2010) ANAIS: analysis of NimbleGen arrays interface. *Bioinformatics* **26:** 2468–2469.

Skaar, E.P. (2010) The battle for iron between bacterial pathogens and their vertebrate hosts. *PLoS Pathog* **6:** e1000949.

Storey, J.D., and Tibshirani, R. (2003) Statistical significance for genomewide studies. *Proc Natl Acad Sci USA* **100:** 9440–9445.

Szklarczyk, D., Franceschini, A., Kuhn, M., Simonovic, M., Roth, A., Minguez, P., *et al*. (2011) The STRING database in 2011: functional interaction networks of proteins, globally integrated and scored. *Nucleic Acids Res* **39:** D561–D568.

Vidakovics, M.L., Lamberti, Y., Serra, D., Berbers, G.A., van der Pol, W.L., and Rodriguez, M.E. (2007) Iron stress increases *Bordetella pertussis* mucin-binding capacity and

attachment to respiratory epithelial cells. *FEMS Immunol Med Microbiol* **51:** 414–421.
de Vries, S., Bootsma, H.J., Hays, J., and Hermans, P.W. (2009) Molecular aspects of *Moraxella catarrhalis* pathogenesis. *Microbiol Mol Biol Rev* **73:** 389–406.
de Vries, S., van Hijum, S.A., Schueler, W., Riesbeck, K., Hays, J., Hermans, P.W., and Bootsma, H.J. (2010) Genome analysis of *Moraxella catarrhalis* strain RH4, a human respiratory tract pathogen. *J Bacteriol* **192:** 3574–3583.
Wang, W., and Hansen, E.J. (2006) Plasmid pWW115, a cloning vector for use with *Moraxella catarrhalis*. *Plasmid* **56:** 133–137.
Wang, W., Reitzer, L., Rasko, D.A., Pearson, M.M., Blick, R.J., Laurence, C., and Hansen, E.J. (2007) Metabolic analysis of *Moraxella catarrhalis* and the effect of selected *in vitro* growth conditions on global gene expression. *Infect Immun* **75:** 4959–4971.
Whitby, P.W., Seale, T.W., Morton, D.J., VanWagoner, T.M., and Stull, T.L. (2010) Characterization of the *Haemophilus influenzae tehB* gene and its role in virulence. *Microbiology* **156:** 1188–1200.

## Supporting information

Additional supporting information may be found in the online version of this article.